Designing Continuous Proximate Time-Optimal Control System for a Class of Third-Order Systems

Samer Charifa, Muammer Kalyon

[1]*Automated Precision, Inc., Samer.charifa@apisensor.com*
[2]*Gebze Institute of Technology, mkalyon@gyte.edu.tr*

Abstract

In this paper, we propose Continuous Proximate Time Optimal (CPTO) control system for a class of third-order systems having an integrator and two stable real roots. The proposed CPTO control system is hybrid and combines the functionality of two controllers, namely, a linear controller and a nonlinear time-optimal controller. The CPTO control system behaves almost like the ideal time-optimal control for large state errors, whereas, for states near the origin, the CPTO control system approximates the linear law. The performance of the control system is tested and the simulation results show near time-optimal response for large state errors, and smooth, stable response with near linear control for small state errors.

Keywords: *Continuous Time-Optimal Control, Hard Disk Drive.*

1. Introduction

If there is a limit on the magnitude of the controller output, a constraint, which exists in almost every control system, and if the servomechanism is time-optimal, the nonlinear controller is generally bang-bang. Unfortunately, time-optimal bang-bang control systems are often impractical because unavoidable measurement noise, disturbances and non-ideal components cause the bang-bang control to switch when the state does not exactly meet the switching criteria, which is obtained from time-optimal control theory. This may degrade tracking performance and produce other undesirable effects such as limit cycles around the target state. In order to reduce or eliminate such an undesirable behavior, a number of nonlinear controllers have been developed in the literature [1-6].

Workman [1], [2] proposed what-so-called Proximate Time-Optimal Servomechanism (PTOS) for double integrator plants. He showed that the controller generates solutions, which approach minimum-time solutions when the system disturbances and modeling errors vanish. The controller approximates the switching curve with a strip such that the optimal switching curve is centered along the strip. Unlike the bang-bang controller, the PTOS controller is continuous in the neighborhood of the strip. Near the origin, the PTOS controller switches to a linear feedback law; in this sense the PTOS controller has dual mode behavior. Similar results have been obtained by Pao and Franklin for two different third-order systems [3], [4].

Ho [5] introduced an alternative dual mode concept by combining time-optimal control and input shaping methods. He used an input shaping technique to account for the flexible dynamics during the entire slewing motion. The feedforward command is derived by shaping the bang-bang input that is based on the open-loop deadbeat control for the pure rigid body system. However, the deadbeat control command does not have an analytical solution, and it is necessary to numerically re-compute the shaped feedforward command for each set point change.

Wu [6] introduced high gain linear state feedback law to achieve minimum-time control based on equivalent switching line, switching plane, and switching hyper plane for a class of second, third, and higher order systems, respectively, provided that feedback coefficients are re-selected for each initial condition. Kim et al. [7] proposed an approach called robust time-optimal control algorithm based on internal loop compensator. They have shown that internal loop compensator isolates the system dynamics from uncertain disturbances including modeling error, external disturbance, shock, and control torque saturation. The mixed sensitivity method is used for optimization of the internal loop compensator.

Recently, La-orpacharapan and Pao developed a shaped time-optimal servomechanism (STOS) control technique [8], [9]. The basic idea of the STOS approach is to start with the time-optimal bang-bang control that moves the rigid body portion of the system from rest to rest and then to shape this control with an input shaper to account for the dominant flexible mode. Moreover, Hu [10], [11] has proposed Time Optimal Unified Servo Controller (TOUSC) as a solution for the HDD time-optimal control problem. This is based on a discrete time-optimal control law. The problem of this type of controllers is that it needs a velocity feedback and in practice this could be very noisy. Choi et al. [12] have proposed Damping Scheduling PTOS (DSPTOS). They have proposed that the damping coefficient for the closed loop system in the DSPTOS are predetermined and do not need complex tuning as in the conventional PTOS. Later on in this paper, we will compare the performance of our proposed Continuous Proximate Time Optimal Control with the performance of the TOUCS and the DSPTOS controllers for 10000 track stroke.

Kalyon [13-16] proposed CPTO control system applied to all second-order systems having plant transfer functions with real roots including unstable roots. Kalyon obtained complete stability proof of all the second-order systems considered. The CPTO controller for a second-order system provides nonlinear operation of the servo within a narrow strip in the neighborhood of the switching curve, and near linear operation in neighborhood of the origin except for small and rapidly diminishing effects of the nonlinear terms. The strip is constructed so that the switching curve is not centered within the strip, but rather the switching curve forms one of the boundaries of the strip. Near the origin the strip is shifted so that it contains the origin in its center.

The objectives of this paper are: (i) Design a novel CPTO-based controller for a class of third-order plants having three real roots, namely, an integrator and two real stable roots; (ii) Apply the developed third-order CPTO controller for track-to-track seek control, which attempts to move read/write head servo systems of hard disk drives from one track to another in almost minimum time; (iii) Analyze stability and performance of the proposed controllers by comparing them with the saturated linear feedback controller through all necessary simulation runs.

This paper is arranged as follows: In Section 2, we describe the mathematical model of the considered class of third-order systems. In Section 3, we design the ideal time optimal controller for the system under consideration. In Section 4, we describe the proposed CPTO controller for the third-order system and show computer simulation results. Moreover, in this section we discuss the robustness of the control system in term of parameter variations. Finally, conclusions are given in Section 5.

2. Mathematical Modeling

A Hard Disk Drive (HDD) is the primary medium for storing information on computers and many other devices, because it combines high capacity, relatively fast access and low price. The hard disk drive is made up of four basic components: a Voice Coil Motor (VCM), a

spinning disk platter, a head arm with a read/write head on its end, and electronics to tie everything together and connect it to the outside world, see Figure 1.

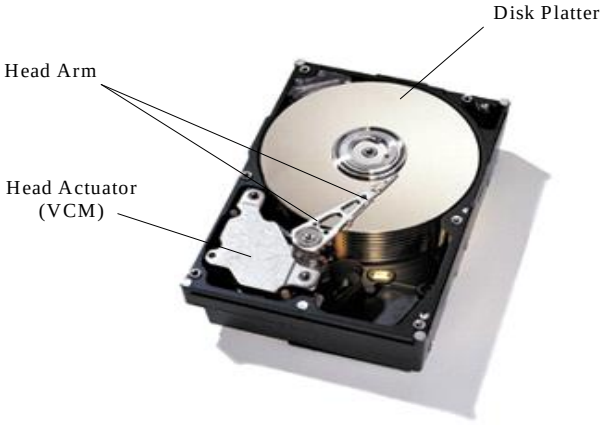

Figure 1. Basic components of the typical hard disk drive.

The read/write head-positioning servomechanism in HDDs has mainly two functions which are track seeking and track following. Track seeking moves the read/write head to the desired track and track following keeps the read/write head on the reference track within minor deflection error while reading/writing [17].

In this paper, we consider the track seeking problem of the HDD. The open loop transfer function from the bounded input u ($u_{\max} = 12$ *Volts*) to the head position $y(m)$ for a typical HDD Read/Write servo mechanism is shown in Figure 2 and given by (considering rigid motion only),

$$\frac{y(s)}{u(s)} = G_p(s) = \frac{rK_t}{JL}\frac{1}{s(s^2 + \frac{R}{L}s + \frac{K_bK_t}{JL})} = \frac{K_0}{s(s+s_1)(s+s_2)}, \tag{1}$$

where,

$$K_0 = \frac{rK_t}{JL}, s_1 = \frac{R}{2L} - \frac{1}{2}\sqrt{\frac{R^2}{L^2} - 4\frac{K_bK_t}{JL}}, \text{and } s_2 = \frac{R}{2L} + \frac{1}{2}\sqrt{\frac{R^2}{L^2} - 4\frac{K_bK_t}{JL}}. \tag{2}$$

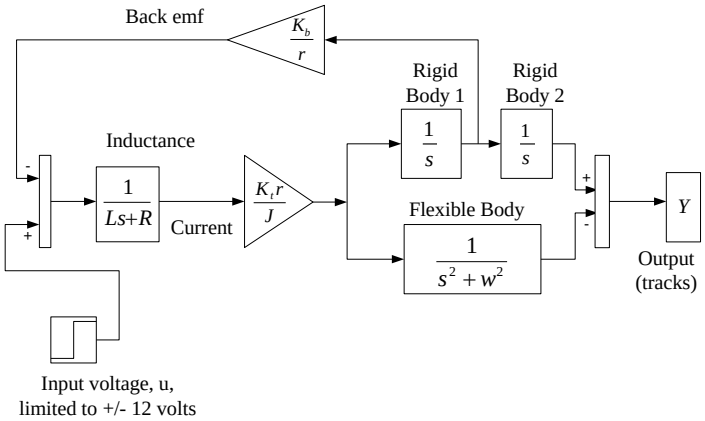

Figure 2. An Open-loop system of a typical HDD head positioning system.

The following denotations have been adopted in this paper:

L : Inductance (Henry).

J : Moment of inertia of the head and head carriage (Kg.m).

r : Length of the head carriage (m).

R : Resistance (ohm).

K_b: Back electromotive force gain (volt.sec).

K_t: Overall armature constant (N.m /A).

The following values are considered acceptable for typical HDD parameters: $L = 10^{-3}$ Henry, $J = 10^{-6}$ Kg.m^2, $r = 0.03$ m, $R = 10$ Ohm, K_t = 0.1 N.m/A, and $K_b = 0.1$ volt.sec. These values correspond to the following parametric values in Eq. (1): $K_0 = 3 \times 10^6$, $s_1 = 1127.0166$, and $s_2 = 8873.9833$. For convenience, we replace two units, namely, unit track (*track*) to replace meter as a position unit and millisecond (*ms*) to replace second as a time unit. Converting all parametric values in Eq. 1 to the new unit system, (this is explained in details in Appendix I), the transfer function for the open-loop system in Eq. 1 can be written as:

$$\frac{y(s)}{u(s)} = G_p(s) = \frac{1.524}{s(s^2 + 10s + 10)} = \frac{1.524}{s(s + 1.127)(s + 8.873)}. \quad (3)$$

The open loop transfer function in Eq. 3 will be integrated in the closed loop system shown in Figure 3.

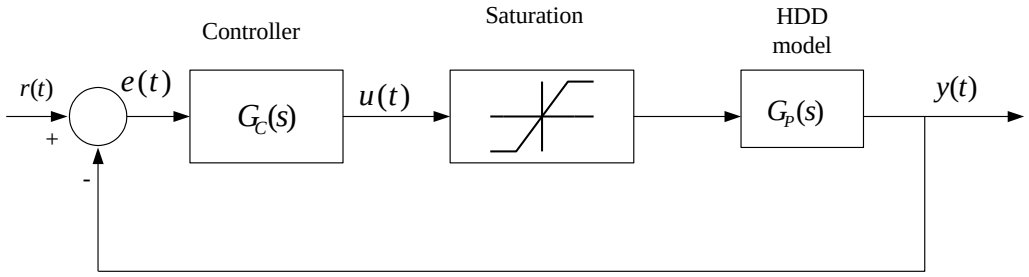

Figure 3. Block diagram of the closed-loop system.

Now, we consider a class of third-order closed-loop systems shown in Figure 3. The saturation function in Figure 3 is defined as,

$$sat(u) = \begin{cases} u_{\max} \operatorname{sgn}(u) & \text{if} \quad |u| \geq u_{\max} \\ u & \text{if} \quad |u| < u_{\max} \end{cases}, \quad (4)$$

where $u_{\max}$ is the maximum control authority. We note that $r(t)$ is the desired head position (reference signal). The state space representation of the system in Figure 3 can be written as follows:

$$\frac{dX(t)}{dt} = A \cdot X(t) + BK_0 u(t), \quad (5)$$

where,

$$X(t)=\begin{bmatrix} x_1(t) \\ x_2(t) \\ x_3(t) \end{bmatrix}, A=\begin{bmatrix} -s_1 & 1 & 0 \\ 0 & s_2 & 1 \\ 0 & 0 & 0 \end{bmatrix}, \text{ and } B=\begin{bmatrix} 0 \\ 0 \\ -1 \end{bmatrix},$$

and where the error-state variables are:

$$x_1(t)=r(t)-y(t),\ x_2(t)=\dot{x}_1(t),\ \text{and } x_3(t)=\dot{x}_2(t). \tag{6}$$

We decouple the system in Equations (5-6) using the following similarity transformation

$$X(t)=P\cdot Z(t), \tag{7}$$

where,

$$Z(t)=\begin{bmatrix} z_1(t) \\ z_2(t) \\ z_3(t) \end{bmatrix},\ P=\begin{bmatrix} 1 & 1 & 1 \\ -s_1 & -s_2 & 0 \\ s_1^2 & s_2^2 & 0 \end{bmatrix} \text{ and, } A=\begin{bmatrix} -s_1 & 1 & 0 \\ 0 & s_2 & 1 \\ 0 & 0 & 0 \end{bmatrix}.$$

The corresponding decoupled system can be written as:

$$\begin{aligned} \frac{d}{dt}Z(t) &= P^{-1}\cdot A\cdot P\cdot Z(t)+P^{-1}\cdot BK_0u(t) \\ &= \begin{bmatrix} -s_1 & 0 & 0 \\ 0 & -s_2 & 0 \\ 0 & 0 & 0 \end{bmatrix}\begin{bmatrix} z_1(t) \\ z_2(t) \\ z_3(t) \end{bmatrix}+\begin{bmatrix} b_1 \\ b_2 \\ b_3 \end{bmatrix}u(t), \end{aligned} \tag{8}$$

where $b_1=K_0/[s_1(s_2-s_1)]$, $b_2=-K_0/[s_2(s_2-s_1)]$ and $b_3=-K_0/(s_1s_2)$. Thus, the decoupled system can be expressed as:

$$\begin{aligned} \tfrac{d}{dt}z_1(t) &= -s_1z_1(t)+b_1u(t), \\ \tfrac{d}{dt}z_2(t) &= -s_2z_2(t)+b_2u(t), \\ \tfrac{d}{dt}z_3(t) &= b_3u(t). \end{aligned} \tag{9}$$

3. Ideal Time Optimal Bang-Bang Control

In this section, we establish a switching criterion for this class of third-order systems. Let τ represents the negative time, as opposed to the positive time t, that is, $t=-\tau$, which implies $\frac{d(\,)}{dt}=-\frac{d(\,)}{d\tau}$. Thus, Eq. (8) can be rewritten as:

$$\begin{aligned} \tfrac{d}{d\tau}z_1(\tau) &= s_1z_1(\tau)-b_1u(\tau), \\ \tfrac{d}{d\tau}z_2(\tau) &= s_2z_2(\tau)-b_2u(\tau), \\ \tfrac{d}{d\tau}z_3(\tau) &= -b_3u(\tau). \end{aligned} \tag{10}$$

The main idea behind backward integrations is that we start with the target error state i.e., the origin $(0,0,0)$, and integrate backward in time towards the initial state. In this regard, firstly, we assume $u(\tau)=\Delta^*$, where $\Delta^*=\pm u_{max}$, for $0\le\tau\le t_1$, where t_1 is the time at which the state hits the switching curve backward in time, secondly, we assume $u(\tau)=-\Delta^*$

for $t_1 \le \tau \le t_2$, where t_2 is the time at which the state hits the switching surface backward in time. In order to obtain t_1 we integrate Eq. (10),

$$\begin{aligned} z_1(\tau) &= \frac{b_1\Delta^*}{s_1}(1-e^{s_1\tau}), \\ z_2(\tau) &= \frac{b_2\Delta^*}{s_2}(1-e^{s_2\tau}), \\ z_3(\tau) &= -b_3\Delta^*\tau. \end{aligned} \tag{11}$$

Since $b_3 < 0,$ it is noted from Eq. (11) that for τ to be positive, Δ^* and z_3 must have the same polarity. Hence, we get:

$$\Delta^* = u_{\max}\ \mathrm{sgn}(z_3), \tag{12}$$

where the *sgn* function is defined as:

$$\mathrm{sgn}(x) = \begin{cases} +1 & \text{if} \quad x > 0, \\ 0 & \text{if} \quad x = 0, \\ -1 & \text{if} \quad x < 0. \end{cases}$$

As a result, the set of equations describing the time-optimal switching curve V_2 can be obtained as:

$$V_2 = \left\{ z\ :\ \begin{array}{c} Z_1(z_3) = \frac{b_1\Delta^*}{s_1}(1-e^{\frac{-s_1 z_3}{b_3\Delta^*}}), \\ Z_2(z_3) = \frac{b_2\Delta^*}{s_2}(1-e^{\frac{-s_2 z_3}{b_3\Delta^*}}). \end{array} \right\}, \text{where } \Delta^* = u_{\max}\ \mathrm{sgn}(z_3). \tag{13}$$

At $\tau = t_1$, we compute the point of the switching curve intersection as:

$$\begin{aligned} z_1(t_1) &= \frac{b_1\Delta^*}{s_1}(1-e^{s_1 t_1}), \\ z_2(t_1) &= \frac{b_2\Delta^*}{s_2}(1-e^{s_2 t_1}), \\ z_3(t_1) &= -b_3\,\Delta^* t_1. \end{aligned} \tag{14}$$

Next, we assume $u(\tau) = -\Delta^*,$ for $t_1 \le \tau \le t_2$ and integrate the set of equations (10),

$$\begin{aligned} z_1(\tau) &= \frac{b_1\Delta^*}{s_1}(2e^{-s_1\tau} - e^{-s_1(\tau-t_1)} - 1), \\ z_2(\tau) &= \frac{b_2\Delta^*}{s_2}(2e^{-s_2\tau} - e^{-s_2(\tau-t_1)} - 1), \\ z_3(\tau) &= b_3\Delta^*(\tau - t_1). \end{aligned} \tag{15}$$

Similar to the process of finding the switching curve, but with lengthy algebra, we find the equation describing the switching surface. This process is described in details in [18]. Thus, the switching surface V_1 can be written as:

$$V_1 : Z_1(z_2, z_3) = -\eta\Delta^*\{[(g(z_2, z_3) - 1)^2 - 1]e^{\frac{s_1 b_3 z_3}{\Delta^*}} + 1\},$$

$$\text{where, } g(z_2, z_3) = \{1 + \sqrt{[1 + (\frac{z_2}{\eta\Delta^*} - 1)e^{-s_2(\frac{z_3}{b_3\Delta^*})}]}\}^{\frac{s_1}{s_2}}, \text{ and } \eta = \frac{-b_3}{\sqrt{1 - 4\left(\frac{1}{s_2} + \frac{1}{s_1}\right)}}. \quad (16)$$

Let, $\Delta t_1 = t_1$ and $\Delta t_2 = t_2 - t_1$, where Δt_1 and Δt_2 represent the time intervals over which the trajectory moves on the switching curve and the switching surface, respectively. From equations (11) and (15), we can write Δt_1 and Δt_2 as:

$$\Delta t_2 = \frac{z_3}{b_3\Delta^*} + \frac{1}{s_2}\ln\{1 + \sqrt{1 - e^{-(\frac{s_2 z_3}{b_3\Delta^*})}(1 - \frac{z_2}{\eta\Delta^*})}\}, \quad (17)$$

$$\Delta t_1 = \frac{1}{s_2}\ln\{1 + \sqrt{1 - e^{-(\frac{s_2 z_3}{b_3\Delta^*})}(1 - \frac{z_2}{\eta\Delta^*})}\}. \quad (18)$$

Here, Δ^* determines the control sequence to reach the state $\mathbf{z} \in V_1$ by moving backwards in time from the origin. For instance, $\Delta^* = +u_{\max}$ means the state can be reached from the origin with the control sequence $\{+u_{\max}, -u_{\max}\}$. Therefore, once Δ^* is determined, then, the control sequence to reach a given state is also determined. In particular, if $\Delta^* = +u_{\max}$, then the control sequence to reach a given state from the origin is $\{\square u_{\max}, \square u_{\max}, \square u_{\max}\}$.
In order for Δt_1 and Δt_2 to be real and positive, we have shown in [18] that Δ^* in the switching surface (16) can be determined using the following relationship:

$$\Delta^* = u_{\max}\,\text{sgn}\{z_2 - Z_2(z_3)\}. \quad (19)$$

Thus, the switching curve and the switching surface can be obtained and shown in figures (4-5).

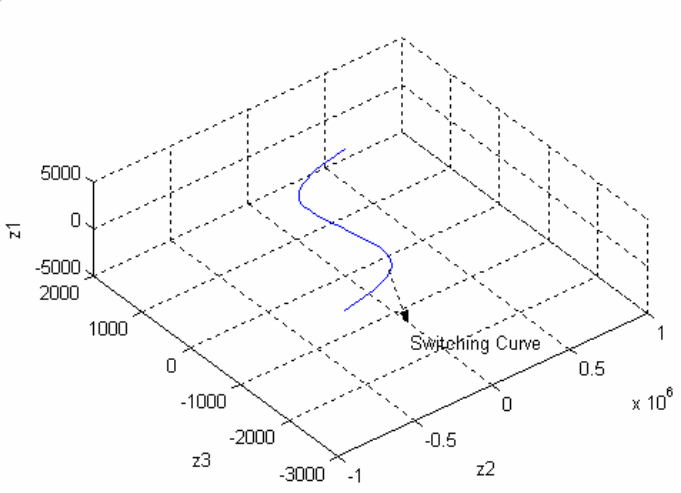

Figure 4. The Switching curve for a class of third order systems.

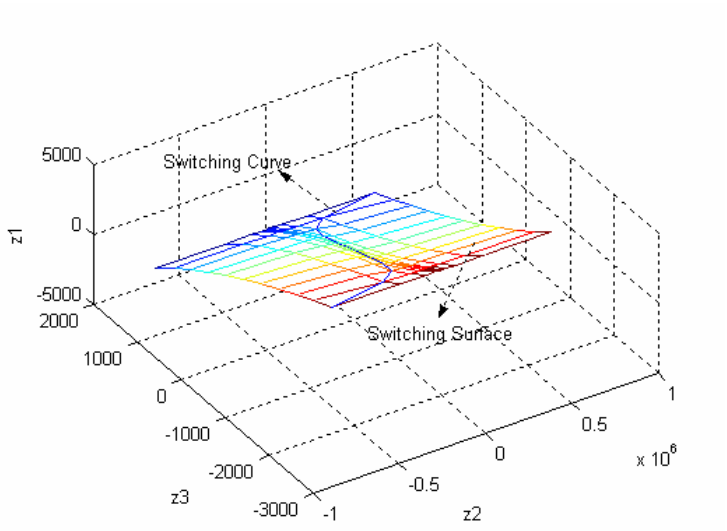

Figure 5. The Switching Surface for a class of third order systems.

In this paper, the switching surface function is denoted as $Z_1(z_2, z_3)$, and the switching curve function is denoted as $\{Z_2(z_3),\ Z_1(z_3)\}$. Thus, we can write the exact time-optimal bang-bang control of the system described in (8) as:

$$U^*(z_1,z_2,z_3)=\begin{cases} u_{\max}\ \mathrm{sgn}[z_1 - Z_1(z_2,z_3)] & \text{if} \quad z_1 - Z_1(z_2,z_3)\neq 0, \\ -u_{\max}\ \mathrm{sgn}[z_2 - Z_2(z_3)] & \text{if} \quad z_1 - Z_1(z_2,z_3)=0 \text{ and } z_2 - Z_2(z_3)\neq 0, \\ u_{\max}\ \mathrm{sgn}(z_3) & \text{if} \quad z_1 - Z_1(z_2,z_3)=0 \text{ and } z_2 - Z_2(z_3)=0. \end{cases} \tag{20}$$

From (20), we recognize three differences cases:
a) The state $\mathbf{z} = [z_1, z_2, z_3]^T$ is not on the switching surface; b) The state is on the switching surface but not on the switching curve; and c) The state is on the switching surface and the switching curve.

4. Continuous proximate time-optimal control

To fix the well-known chattering problem found in the ideal time-optimal control law described in Eq. (20), we propose the following CPTO control law:

$$U(z_1,z_2,z_3)=sat\{k_1\{[z_1 - Z_1(z_2,z_3)] - \frac{1}{k_1} sat\{k_1k_2[z_2 - Z_2(z_3)] - sat(k_1k_3z_3)\}\}\}. \tag{21}$$

The control system described in (20) is a continuous state feedback controller implemented on the servo system of the HDD.

Claim 1: Considering equations (13-21),

$$U(z_1,z_2,z_3)\to U^*(z_1,z_2,z_3),\ \text{ as }\ k_1\to\infty;\ \forall(z_1,z_2,z_3)\neq 0. \tag{22}$$

The detail proof of Claim 1 is given in [18].

Claim 2: Considering equations (13-21),

$$U(z_1, z_2, z_3) \to U_L(z_1, z_2, z_3) = \hat{k}_1(z_1 + \hat{k}_2 z_2 + \hat{k}_3 z_3), \text{ as } (z_1, z_2, z_3) \to 0. \tag{23}$$

Note from (21) that as $(z_1, z_2, z_3) \to 0$, all the "sat" functions in (21) are unsaturated, which yields:

$$U(z_1, z_2, z_3) = k_1[z_1 - Z_1(z_2, z_3)] - k_1 k_2[z_2 - Z_2(z_3)] + k_1 k_2 z_3. \tag{24}$$

Linearization of the functions $Z_1(z_2, z_3)$ and $Z_2(z_3)$ around $(z_1, z_2, z_3) \to 0$, respectively, yields:

$$Z_1(z_2, z_3)\big|_{z \to 0} \cong -\frac{s_1^2}{s_2^2} z_2 - \frac{s_1^2}{\eta}(s_2 - s_1) z_3, \tag{25}$$

$$\text{and } Z_2(z_3)\big|_{z \to 0} \cong \frac{s_2^2 s_1}{\eta} z_3.$$

Substituting (25) into (24) and organizing,

$$U(z_1, z_2, z_3) = \hat{k}_1(z_1 + \hat{k}_2 z_2 + \hat{k}_3 z_3), \tag{26}$$

where,

$$\hat{k}_1 = k_1, \quad \hat{k}_2 = \frac{s_1^2}{s_2^2} - k_2, \quad \text{and} \quad \hat{k}_3 = k_3 + k_2 \frac{s_2^2 s_1}{\eta} + s_1^2.$$

In Eq. (26), we have obtained relations relating the gain constants of the CPTO controller and the gain constants of the linear controller. Note that the linear controller will take over from the CPTO controller when $(z_1, z_2, z_3) \to 0$.

4.1. Designing the Controller Gains for the Third-Order System

Since the CPTO controller converges to the linear controller when the state is small, computation of controller gains is an integral part of CPTO controller design. We use the following design criterion for track following and track seeking; (i) Percent Overshoot (PO) $\leq 10\%$; (ii) The settling time (t_s) equals 1 ms ; (iii) The error for the assumed settling time must be less than 10%.

To find the closed-loop poles of the system, we apply Pole Placement Method. We get the following values for the poles,

$$p_1 = -12.9084 + 17.6649i, \; p_2 = -12.9084 - 17.6649i, \text{ and } p_3 = -120.$$

The linear controller constants can be written as,

$$k_1 = 27687, \; k_2 = 0.011, \text{ and } k_3 = 1.3613.$$

Substituting these values into (26), we get the gain constants of the CPTO controller as follows

$$\hat{k}_1 = 27687, \; \hat{k}_2 = 0.0322, \text{ and } \hat{k}_3 = 0.0051.$$

4.2. Simulation Results

The performance of the CPTO controller with the initial condition $X(0) = [1{,}000 \quad 0 \quad 0]^T$, and $[10{,}000 \quad 0 \quad 0]^T$ tracks is shown in figure 6 and 7. Clearly, all the state variables converge to zero and remain there. The settling time is less than 1.25 and 4.5 *ms* for the 1000 and 10^4 *track* where the settling time error is less than 0.1 *track*. In figures (6-7), we compare the CPTO with the Ideal Proximate Time-Optimal (IPTO) control. Clearly, the CPTO performance is near optimal with the difference is that the switching between the two modes of control is smooth compare to the sharp switching of the IPTO, as illustrated in Figure 8.

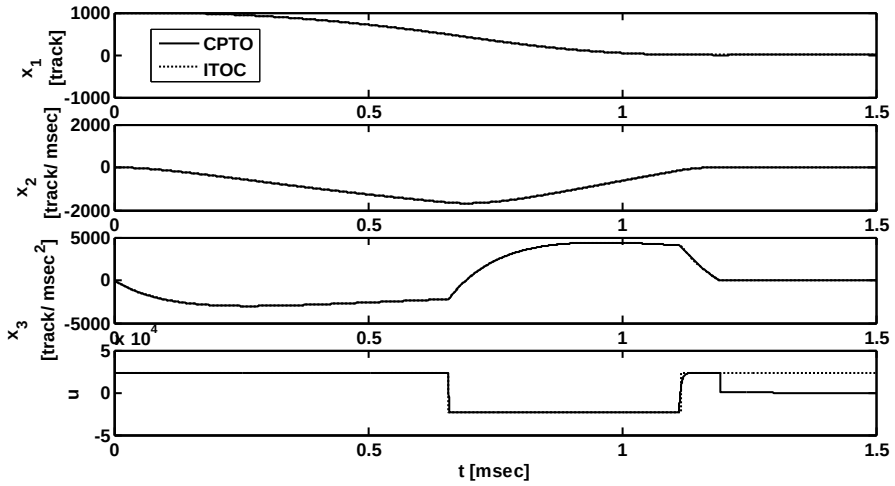

Figure 6. The response of the CPTO Controller for 1000 tracks.

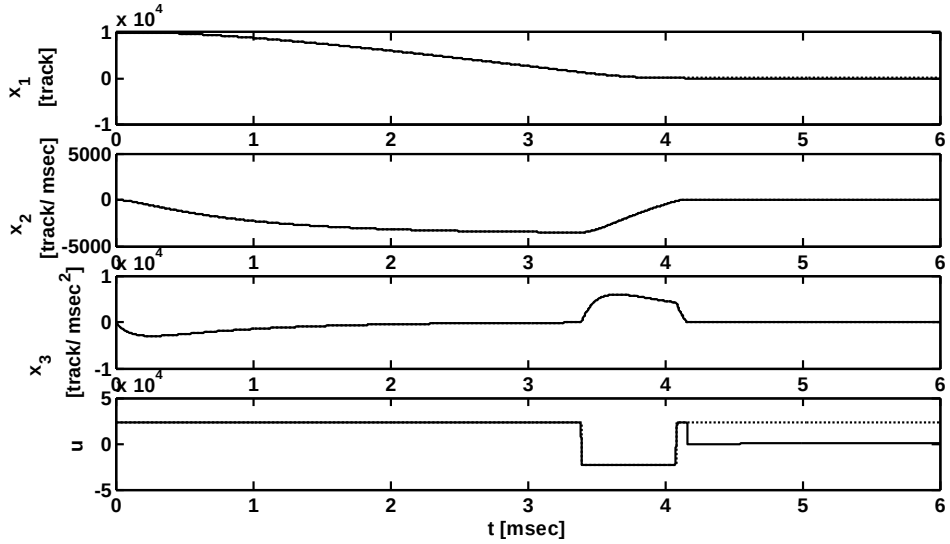

Figure 7. The response of CPTO controller for 10,000 tracks.

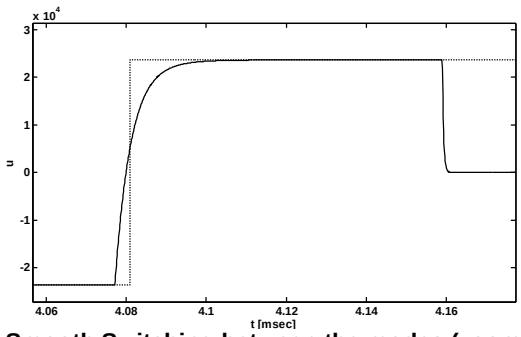

Figure 8. Smooth Switching between the modes (zoomed section of Figure 7).

4.3. Robustness of the CPTO Controller to Parameter Variations

The motivation behind the robustness to variation analysis is due to the fact that actual system parameters often differ from the nominal values used in the controller design. Let us examine first the effect of changing the plant gain constant K_0, Eq. (5), on the performance of the proposed CPTO control law Eq. (21). Assume that the actual plant gain constant is k_a, and the controller is designed for nominal plant gain constant $k_n \neq k_a$. Let us compare how much the performance of the proposed CPTO controller degrades as k_a deviates from k_n. Thus, we have the following two cases:

Case I: Assume $k_n < k_a$, which means that there is less effective control than the nominal control effort. Note that from Eq. (5) that the plant gain constant is multiplied by the control effort. Figure 9 shows the error state-response with initial condition $X(0) = [1000 \quad 0 \quad 0]$ for a CPTO controller having parameter variation of $k_a = 0.8k_n$. We note from Fig. 9 that the trajectory converges to the origin after overshooting two times. Evidently, the response time is greater than the response time of the plant with no parameter variation. The control history, shown in Fig. 10, shows no chattering. Here, we will report than on testing the control system for $k_a = 0.7k_n$, the system failed to reach the origin. To solve this problem, we conclude that the control law should be designed for $k_a = k_n - d_\infty$, where d_∞ is the maximum positive uncertainty in the plant gain constant. Designing the control law in this manner is considered in [13], where it is called worst-case analysis.

Note that in Figures 7-13 the control signal is in [$\frac{track^2}{A.ms^3}$], see Appendix I.

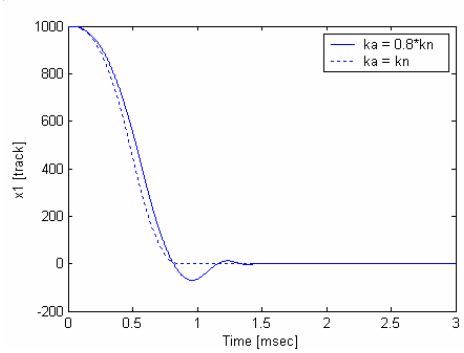

Figure 9. The response of the HDD system having $K_a = 0.8K_n$.

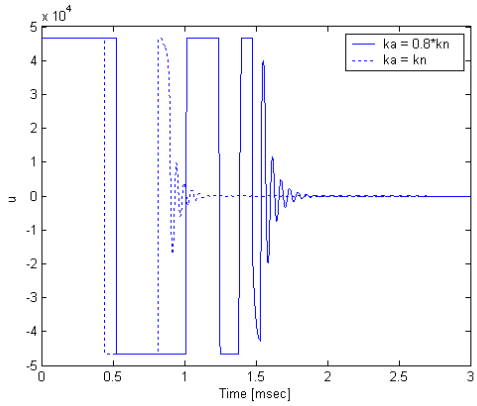

Figure 10. The CPTO control history for $K_a = 0.8K_n$.

Case II: Assume that $k_a > k_n$. There is more effective control than the nominal control effort. In figures 11-14, the system is tested for the cases where $k_a = 1.2k_n$ and $k_a = 1.4k_n$. It is shown from figures (11-14) that the CPTO control has faster response for an increasing gain constant than the response with a nominal gain constant. We further conclude that the designed CPTO controller is reasonably robust for the variations in plant gain constant.

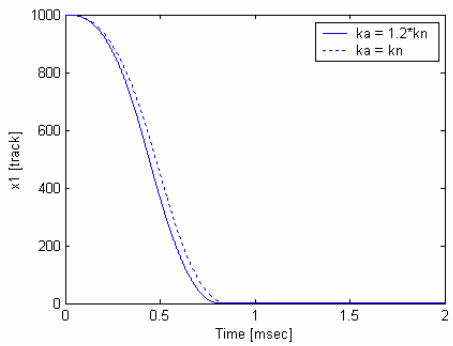

Figure 11. The response of the HDD system having parameter variation of $K_a = 1.2K_n$.

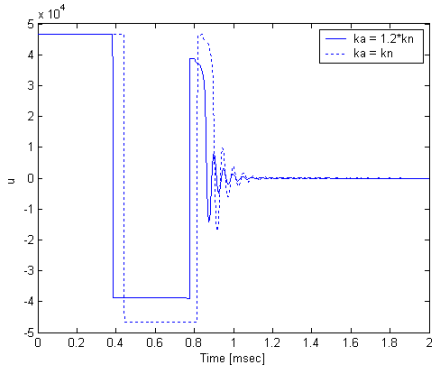

Figure 12. The control histories of the CPTO controller and the ITOC for a system with $K_a = 1.2K_n$.

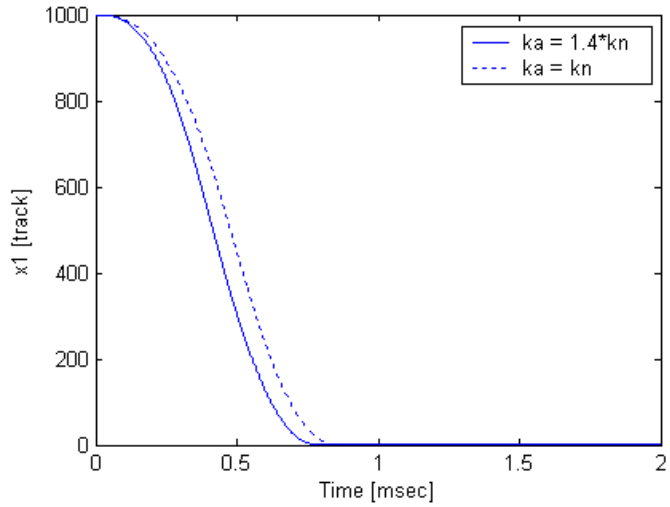

Figure 13. The response of the HDD system for the case $K_a = 1.4K_n$.

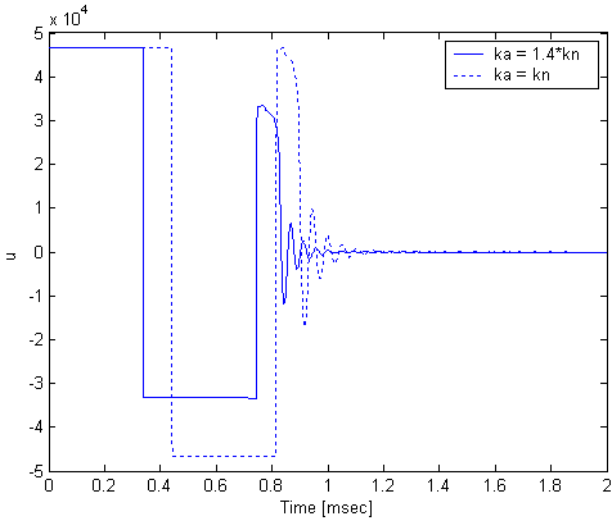

Figure 14. The control histories of the CPTO controller and the ITOC for the case $K_a = 1.4K_n$.

5. Conclusions

In this paper, we have developed CPTO controllers for a class of third-order systems. The third-order CPTO control system behaves almost like the ideal third-order time-optimal control for the large state errors and, for the error states near the origin, the CPTO control system law approximates the linear law where the gain constants of the linear controller can be chosen based on linear system design methodology. As an application, we have, successfully, applied the third-order CPTO controller to the HDD servomechanism. For the performance analysis, the response of the each CPTO controller is evaluated by comparing it with the performance of the conventional saturated linear control through the simulation results. It has been shown that the CPTO controller has superiority over the saturated linear controller for large initial states. As a robustness analysis, robustness to parameter variation is examined by considering the most significant parameter, namely, the plant gain constant.

Appendix I: Change of Units:

We note that throughout the paper, we have adopted: ms = millisecond as a unit of time and $track$ as unit of length. Therefore, the following change of unit is necessary:

$$1\,meter = 39.37\,in. = 39.37*(50000)track = (1.9685)*10^6 track,$$

$$1\,Henry = 1\,kgm^2/(A^2 s^2) = 1kg(1.9685)^2*10^{12}track^2/(A^2 10^6 (ms)^2)$$
$$= 3.875*10^6 track^2/(A^2 (ms)^2),$$

$$1\,Ohm = 1\,kgm^2/(A^2 s^3) = 1kg(1.9685)^2*10^{12}track^2/(A^2 10^9 (ms)^3)$$
$$= 3.875*10^3 track^2/(A^2 (ms)^3),$$

and,

$$1Volt = 1\,kgm^2/(As^3) = 1kg(1.9685)^2*10^{12}track^2/(A10^9 (ms)^3)$$
$$= 3.875*10^3 track^2/(A(ms)^3).$$

Using these units, the parameters L, J, r, R, and K_t will have the following new units:

$$L = 10^{-3}\ Henry = 3.87499225*10^3 track^2/(A^2 (ms)^2),$$

$$J = 10^{-6}\ Kgm^2 = 10^{-6} kg(1.9685)^2*10^{12}track^2 = 3.87499225*10^6 kg.track^2,$$

$$r = 0.03m = 3*10^{-2}*1.9685*10^6 track = 5.9055*10^4 track,$$

$$R = 10\,ohm = 3.87499225*10^4 track^2/(A^2 (ms)^3),$$

$$K_t = 0.1\,Nm/A = 0.1kgm^2/(s^2 A) = 0.1kg(1.9685)^2*10^{12}track^2/(10^6 (ms)^2 A)$$
$$= 3.875*10^5 kg*track^2/((ms)^2 A).$$

Acknowledgement

The authors would like to thank Saudi Basic Industries Corporation (SABIC) for the support of this work (contract: FAST-2005/A).

References

[1] M.L. Workman, "Adaptive Proximate Time-Optimal Servomechanisms: Continuous Time Case," American Control Conference, Minneapolis, MN, 1987, pp. 589-594.

[2] M.L. Workman, "Adaptive Proximate Time-Optimal Servomechanisms," Ph.D. dissertation, Stanford University, 1987.

[3] L.Y. Pao, and G.F. Franklin, "Proximate Time-Optimal Control of Third-Order Servomechanisms," IEEE Transactions on Automatic Control, 38, 1993, pp. 560-580.

[4] L.Y. Pao, and G.F. Franklin, "Design for Robust Controls Having Almost Minimum Time Response," American Control Conference, Chicago, IL, 1992.

[5] H.T. Ho, “Fast servo bang-bang seek control,” IEEE Transactions on Magnetics, 33, 1997, pp. 4522-4527.

[6] Wu, S-T., “Time-Optimal Control and High-Gain Linear State Feedback,” Int. J. of Control, 72, 1999, pp. 764-772.

[7] B.K. Kim, W.K. Chung, and H.S. Lee, "Robust time optimal controller design for hard disk drives," IEEE Transactions on Magnetics, 35, No. 5, 1999, pp. 3598-3600.

[8] C. La-orpacharapan, and L. Y. Pao, "Shaped phase--plane control for disk drive systems with back EMF, slew rate limits, and different acceleration and deceleration rates," in Proc. Amer. Control Conf., Denver, CO, June 2003, pp. 3077--3082.

[9] L.Y. Pao, and C. La-orpacharapan, “Shaped time-optimal feedback controllers for flexible structures”, ASME J. Dyn. Sys. Meas., Control, Dec. 2003.

[10] S. Hu, "On High Performance Servo Control Algorithms for Hard Disk Drive", Doctoral Dissertation, Cleveland State University, 2001.

[11] S. Hu, and Z. Gao, "A Discrete Time Optimal Control Solution for Hard Disk Drives Servo Design," 22nd IEEE International Symposium on Intelligent Control, Singapore, Oct. 2007, pp. 289-295.

[12] Y.-M. Choi, J. Jeong, and D.-G. Gweon, "A Novel Damping Scheduling Scheme for Proximate Time Optimal Servomechanisms in Hard Disk Drives," IEEE Transactions on Magnetics, 42, No. 3, March 2006, pp. 468-472.

[13] M. Kalyon, "Continuous Proximate Time-Optimal Control of Servomechanisms," Ph.D. dissertation, University of Michigan - Ann Arbor, 1993.

[14] M. Kalyon, "Continuous Proximate Time-Optimal Control of an Aerodynamically Unstable Rocket," Journal of Guidance, Control, and Dynamics, 20, 1997, pp. 1049-1052.

[15] M. Kalyon, "Design of Continuous Time Controllers Having Almost Minimum Time Response," ASME J. Dyn. Syst. Meas. Control, 124, June, 2002, pp. 252-260.

[16] M. Kalyon, "Near Minimum Time Optimal Track-to-track Seek Control of HDD by Continuous Proximate Time-Optimal Control", Mechatronics Forum International Conference, Ankara, Turkey, Aug., 2004, pp. 45-57.

[17] B.M. Chen, T.H Lee, K. Peng, and V. Venkataramanan, "Hard Disk Drive Servo Systems," Advances in Industrial Control, 2nd Edition, Springer-Verlag, London, UK, 2006.

[18] M.S. Charifa, "Continuous Proximate Time-Optimal Control for a Third-Order Servomechanism Having a Plant with Three Real Roots," M.S. Thesis, King Fahd University of Petroleum & Minerals, 2005.

Authors

Dr. Samer Charifa

Dr. Charifa received his BS and MS degrees both in Mechanical Engineering in 2001 and 2005, from the University of Aleppo and King Fahd University of Petroleum and Minerals, respectively. In 2009, he received his PhD in Electrical Engineering from North Carolina A & T State University. Currently, he is a senior software engineer at Automated Precision, Inc., Rockville, MD. His current research includes Control Systems and Computer Vision.

Dr. Muammer Kalyon

Dr. Kalyon received his BS degree from Istanbul Technical University, Department of Aeronautical engineering in 1985, MS and PhD degrees from The University of Michigan, Aerospace Engineering Department in 1988 and 1993, respectively. Currently, is a professor of Mechanical Engineering Department at Gebze Institute of Technology, Turkey.